PHYSICAL REVIEW D VOLUME 22, NUMBER 11 1 DECEMBER 1980

Measurement of the K_L^0 form factors from $K_L^0 \to \pi\mu\nu$ decays in the 12-foot bubble chamber

Y. Cho, M. Derrick, R. J. Miller,* and J. Schlereth
Argonne National Laboratory, Argonne, Illinois 60439

A. Engler, G. S. Keyes,† R. W. Kraemer, and M. Tanaka‡
Carnegie-Mellon University, Pittsburgh, Pennsylvania 15213

(Received 15 May 1980)

We report results of a measurement of the form factors in K_L^0 leptonic decay. We analyze both the Dalitz plot of the decay $K_L^0 \to \pi\mu\nu$ and the branching ratio $\Gamma(K_{\mu3}^0)/\Gamma(K_{e3}^0)$. The experiment was performed in the Argonne 12-foot bubble chamber exposed to a monoenergetic K_L^0 beam. Simultaneous detection of $\pi\mu\nu$ and $\pi e\nu$ decays with large acceptance results in well understood systematic uncertainties. The results have been analyzed to give λ_+ and λ_0, the expansion parameters of the form factors dominated by 1^- and 0^+ K^* poles, respectively. From our branching-ratio measurement of $\Gamma(K_{\mu3}^0)/\Gamma(K_{e3}^0) = 0.702 \pm 0.011$, we obtain $\lambda_0 = 0.041 \pm 0.008$. A fit to the $K_{\mu3}^0$ Dalitz-plot density distribution gives $\lambda_0 = 0.050 \pm 0.008$ and $\lambda_+ = 0.028 \pm 0.010$. These numbers are in agreement with our analysis of the K_{e3}^0 decay Dalitz plot and with other recent measurements. A combined fit to all of our data yields $\lambda_+ = 0.028 \pm 0.007$ and $\lambda_0 = 0.046 \pm 0.006$.

I. INTRODUCTION

This paper reports the results of an experiment to measure the K_L^0 form factors. We used two techniques: The first was an analysis of the density of events on the Dalitz plots and the second a measurement of the $K_{\mu3}^0/K_{e3}^0$ branching ratio. The $K_{\mu3}^0$ decay analysis complements our previously reported measurement of the K_{e3}^0 decays observed in the same experiment.[1] There have been numerous previous measurements of the form factors, but since the experiments are difficult and systematic errors are often dominant, the results do not always agree.[2,3] Experiments using counter techniques normally have good particle identification and high statistics, but have low and nonuniform acceptance across the Dalitz plot and therefore rely heavily on Monte Carlo corrections. Bubble-chamber experiments, on the other hand, provide uniform acceptance, but particle identification is poor and the number of events is often small. The use of K_L^0 beams introduces an additional complication in that if the beam momentum is not known, there is a two-fold ambiguity for placing an event of a given decay mode on the Dalitz plot. Our experiment used a low-energy monochromatic beam, which eliminated the twofold fitting ambiguity. Our detector, consisting of a large volume bubble chamber, provided relatively good particle identification. We thus obtained high and uniform acceptance over both the K_{e3}^0 and $K_{\mu3}^0$ Dalitz plots. Analysis of K_{e3}^0 and $K_{\mu3}^0$ in a consistent manner in the same experiment further reduced systematic effects.

II. PHENOMENOLOGY

Assuming the current-current picture of semileptonic K_L^0 decay, we can write the decay matrix element as

$$M = \frac{G}{\sqrt{2}} \sin\theta_C \,[f_+(q^2)(p_K + p_\pi)^\mu \bar{u}_l \gamma_\mu (1+\gamma_5) u_\nu + f_-(q^2)(p_K - p_\pi)^\mu \bar{u}_l \gamma_\mu (1+\gamma_5) u_\nu],$$

where f_+ and f_- are the vector form factors, which are real functions of q^2 only. Tensor and scalar terms do not contribute to the decay in a V-A theory. The density of events on the Dalitz plot is then

$$\frac{d^2N(T_\pi, T_l)}{d\Gamma_\pi \, d\Gamma_l} = \frac{G^2 \sin^2\theta_C}{4\pi^3} \,(Af_+^2 + Bf_+f_- + Cf_-^2)$$

with

$$A = M_K(2T_l T_\nu - M_K T_\pi) + m_l^2(\tfrac{1}{4} T_\pi - T_\nu),$$

$$B = m_l^2(T_\nu - \tfrac{1}{2} T_\pi'),$$

$$C = \tfrac{1}{4} m_l^2 T_\pi',$$

where T stands for the center-of-mass kinetic energy and

$$T_\pi' = T_\pi^{\max} - T_\pi .$$

The quantities q^2 and T are related by

$$q^2 = (M_K - m_\pi)^2 - 2M_K T_\pi .$$

More recent analyses have chosen a different combination of the form factors called f_+ and f_0 expanding them in q^2/m_π^2 as below:

$$f_+(q^2) = f_+(0)\,(1 + \lambda_+ q^2/m_\pi^2),$$

$$f_0(q^2) = f_0(0)(1 + \lambda_0 q^2/m_\pi^2).$$

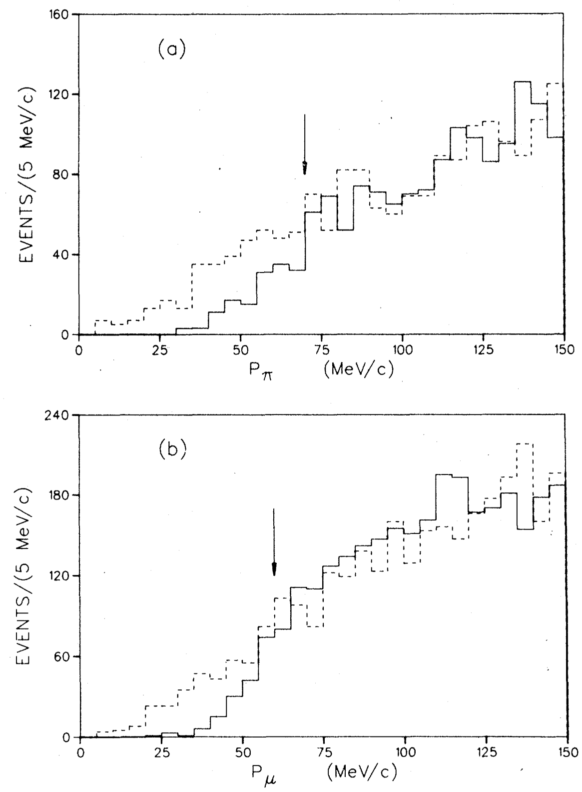

FIG. 1. (a) The distribution of laboratory momenta of the pions in the decay $K_L^0 \to \pi\mu\nu$. The solid curve represents the original distribution and the dashed curve the randomized decay distribution as described in the text. The arrow indicates the value at which we cut. (b) The same as (a) but for muon momenta.

With this parametrization and retaining first terms of the expansion, we get

$$f_0 = f_+ + \frac{q^2}{M_K{}^2 - m_\pi{}^2} f_- ,$$

where f_- has no q^2 dependence. The advantage of this parametrization is that if the form factors obey dispersion relations with, at most, one subtraction, and if in addition the form factors are dominated by K^* poles, then f_+ and f_0 can be related to the K^* mesons which have spin-parity 1^- and 0^+, respectively.

If the $f_+(q^2)$ amplitude is indeed unsubtracted and the dispersion integral is approximated by the K^* pole, then

$$f_+(q^2) = f_+(0)\,\frac{M_{K^*}{}^2}{(M_{K^*}{}^2 - q^2)} ,$$

where M_{K^*} is the mass of the $K^*(890)$, the lowest-mass 1^- K^* meson. This leads to a prediction for λ_+ of $m_\pi{}^2/M_{K^*}{}^2 = 0.025$. Similarly, for the scalar form factor, the model predicts $\lambda_0 = m_\pi{}^2/M_{K^*(1350)}{}^2$ since the $K^*(1350)$ is the lowest 0^+ strange meson. Thus, λ_0 is expected to be smaller than λ_+ in this approximation. The existence and properties of the $K^*(1350)$ are not completely established,[3] but all solutions favor a wide resonance for which a simple pole approximation may not be valid. The prediction of Callan and Treiman,[4] based on current algebra, place the value of λ_0 near 0.02 assuming a linear extrapolation to the unphysical point $q^2 = M_K{}^2$. A detailed discussion of theoretical questions related to leptonic K decay can found in the review of Chounet *et al.*[5]

The parameters λ_+ and λ_0 can be obtained by directly fitting the $K_{\mu3}$ Dalitz-plot density. In our experiment a more accurate measurement of λ_0 can be made, assuming μ-e universality, by fixing λ_+ at the value found from analysis of the K_{e3}^0 Dalitz plot and measuring the branching ratio $\Gamma(K_{\mu3}^0)/\Gamma(K_{e3}^0)$.

III. EXPERIMENTAL DETAILS

Approximately 300 000 pictures were taken in the Argonne National Laboratory 12-foot hydrogen bubble chamber exposed to a 550 ± 35 MeV/c K_L^0 beam. Details of the experimental arrangement have already been presented.[1,6,7] A scan for two-prong events, which correspond to K_L^0 decays, yielded about 45 000 events which were measured, reconstructed, and fitted to the following decay hypotheses:

(a) $K_L^0 \to \pi^+\pi^-\pi^0$,

(b) $K_L^0 \to \pi^\pm e^\mp \nu$,

(c) $K_L^0 \to \pi^\pm \mu^\mp \nu$.

After two measurement passes, 95% of the candidates gave satisfactory fits to one or more of these channels. The remaining events were attributed to decays of scattered K_L^0's and K_L^0 interactions in which the recoil particle was not seen.[7]

The average scanning efficiency for $K_{\mu3}^0$ events was measured to be 0.90 ± 0.01. Scanning losses occur when the π or μ interacts or decays close to the K_L^0 decay vertex. Losses also occur if one of the decay products has very low momentum or is nearly parallel to the magnetic field. These losses have been studied using the following technique. Each reconstructed event is transformed into the K_L^0 rest frame, rotated by a random angle and transformed back to the laboratory frame. The distributions of laboratory momenta obtained in this way are compared to the original distributions in Fig. 1. The data show a deficit of events if $p_\pi < 70$ MeV/c or $p_\mu < 60$ MeV/c. These losses

TABLE I. Cuts and weights for unique events.

Final state	Cuts	Average weight
$K_L^0 \to \pi\mu\nu$	$p_\pi > 70$ MeV/c $p_\mu > 60$ MeV/c $l_{\pi,\mu} > 8$ cm	1.21
$\pi e\nu$	$p_\pi > 70$ MeV/c $p_e > 50$ MeV/c $l_{\pi,e} > 8$ cm $T_e > 40$ MeV/c	1.15

are corrected by cutting the data sample at these values and weighting the remaining events by a compensating factor in the same manner as was used for our K_{e3}^0 events.[1] Table I summarizes the cuts and average weights for a sample of uniquely identified events.

After making these corrections, the scanning and measuring efficiencies were studied as functions of T_π and T_μ. They are very nearly constant as shown in Fig. 2 and averaged about 94%. We have fit these efficiencies for each of the semileptonic decay channels to functions linear in T_π,

$$\epsilon_{SM} = \epsilon_0 + \alpha T_\pi \ .$$

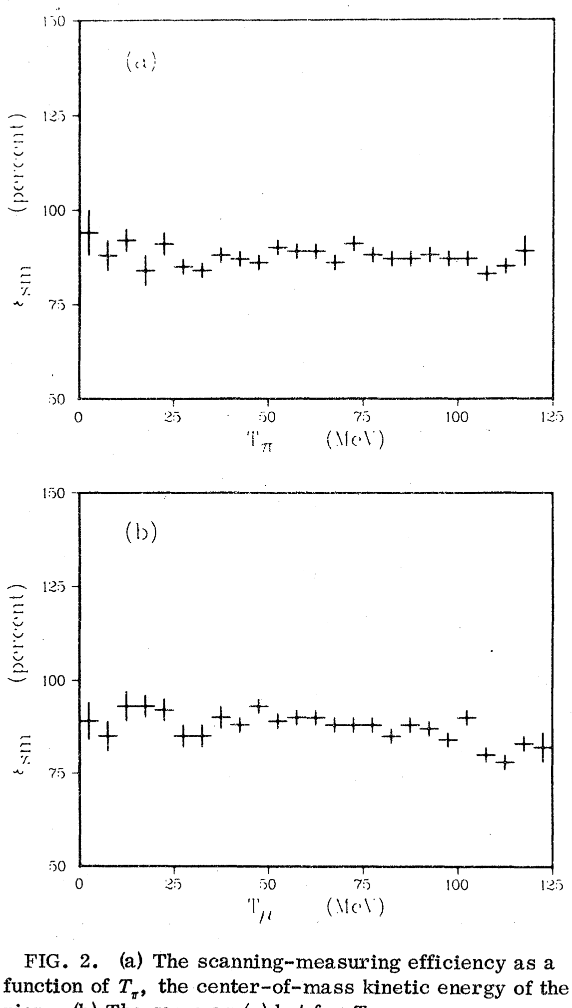

FIG. 2. (a) The scanning-measuring efficiency as a function of T_π, the center-of-mass kinetic energy of the pion. (b) The same as (a) but for T_μ.

TABLE II. Parametrization of the scan-measure efficiencies.

Final state	ϵ_0	α (MeV^{-1})
$\pi^+\mu^-\nu$	0.940	−0.000 41
$\pi^-\mu^+\nu$	0.933	−0.000 33
$\pi^+e^-\nu$	0.949	−0.000 33
$\pi^-e^+\nu$	0.926	−0.000 11

The parameters, listed in Table II, have been applied to subsequent analysis.

Since the K_L^0 beam angles and momentum are known, the fits to reactions (a)–(c) are kinematically constrained. Also, because of the large bubble-chamber volume, many of the particles from the decays could be identified visually via interactions, decays or stops.[1] The $K_{3\pi}$ events are cleanly separated from the semileptonic decays and are not a significant source of background.[6] However, even after fitting and visual classification, a significant number of the events have ambiguous semileptonic decay assignments. The event classification and ambiguities are summarized in Table III.

Of the candidates for the $K_{\mu 3}^0$ decay sample, 53% are ambiguous with either K_{e3}^0 or the opposite charge $K_{\mu 3}^0$ mode or both. This is to be compared with only 37% ambiguous in the K_{e3}^0. In our analysis of K_{e3}^0 decay,[1] we used only the unique events for measurement of the form factor f_+ and Monte Carlo techniques were used to calculate the correction factors. This was possible since most of the ambiguous events are actually $K_{\mu 3}^0$ decays and the fraction of unique K_{e3}^0 events was reasonably uniform across the Dalitz plot. If we were to use this same procedure on the $K_{\mu 3}^0$ events, not only would we be left with a smaller sample, but systematic distortion of the data would be more of a problem since a larger fraction of the events would be discarded. Therefore, we use a different method of analysis which combines both the unique and the weighted ambiguous events.

IV. ANALYSIS PROCEDURE

The ambiguous events are assigned to the different channels according to calculated weights. In order to determine these weights, we make use of necessary constraints. The first is that the

TABLE III. Events fitting K_L^0 decay channels.

Final state	Unique	Ambiguous with other semileptonic decay modes	Ambiguous with opposite charge within $\pi\mu\nu$ or $\pi e \nu$ channels only	Ambiguous with other semileptonic modes and opposite charge
$\pi^+\mu^-\nu$	3570	2599	451	2592
$\pi^-\mu^+\nu$	3299	2041		
$\pi^+e^-\nu$	6718	2981	508	1967
$\pi^-e^+\nu$	6547	2284		

distribution of $\cos\theta_l^*$, the angle of the lepton in the K_L^0 decay frame, must be isotropic. The second is that the charge ratio $\pi^+l^-\nu/\pi^-l^+\nu$ be unity in all regions of the Dalitz plots (within a small known asymmetry). Figure 3 shows the $\cos\theta_l^*$ distribution for the two semileptonic modes separately for unique events (full line) and ambiguous events (dashed line). The ambiguous events must be assigned either to the $\pi e \nu$ hypothesis or to the $\pi\mu\nu$ hypothesis in order to fill in the hole at positive $\cos\theta_l^*$ values seen for the unique event samples.

These assignments are done independently for different regions of the Dalitz plots. The events in each channel were divided into bins of T_π and and T_l, and the $\cos\theta_l^*$ distributions for both the unique and ambiguous events were made. Then we assigned weights to the ambiguous events so that for each value of $\cos\theta_l^*$ some fraction of the ambiguous events plus the unique events were a constant independent of $\cos\theta^*$. That is, we required

$$U_1+wA_1=U_2+wA_2=\cdots=U_N+wA_N\ ,$$

where the subscripts refer to the ith bin in $\cos\theta_l^*$, and we had the additional condition that

$$\sum_{i=1}^{N}\frac{(U_i+wA_i)}{N}=\langle U\rangle+w\langle A\rangle\ ,$$

where $\langle U\rangle$ and $\langle A\rangle$ are the averages over $\cos\theta_l^*$. This implies $(\langle U\rangle-U_i)+w(\langle A\rangle-A_i)=0$ for each i. Thus, we minimized the quantity

$$\chi^2=\sum_i[\delta U_i^e(T_\pi,T_e)+w_e(T_\pi,T_e)\delta A_i^e(T_\pi,T_e)]^2+[\delta U_i^\mu(T_\pi,T_\mu)+(1-w_e)\delta A_i^\mu(T_\pi,T_\mu)]^2\ ,$$

where

$$\delta U_i=\langle U\rangle-U_i\ ,$$
$$\delta A_i=\langle A\rangle-A_i\ .$$

We obtained a weight to be applied to ambiguous events which is a function of T_π and T_l given by

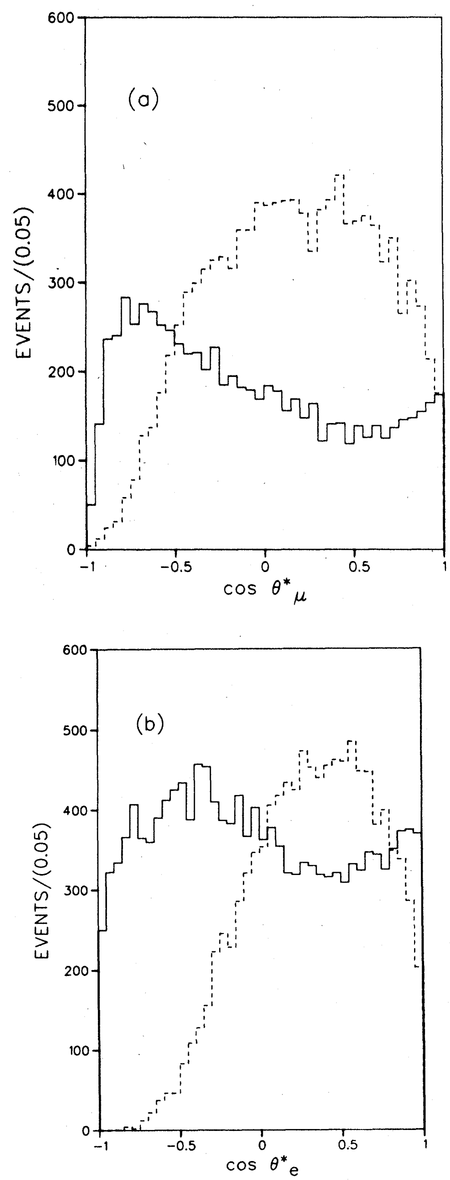

FIG. 3. (a) The distribution of $\cos\theta_\mu^*$, the angle between the μ and the K_L^0 in the center of mass. The solid curve represents the unique events and the dashed curve the ambiguous. (b) The same as (a) but for $\cos\theta_e^*$.

$$w_e(T_\pi, T_l) = \frac{\langle \delta U^\mu \delta A^\mu \rangle - \langle \delta U^e \delta A^e \rangle + \langle \delta A^\mu \delta A^\mu \rangle}{\langle \delta A^e \delta A^e \rangle + \langle \delta A^\mu \delta A^\mu \rangle}$$

and $w_\mu = (1 - w_e)$.

We note that the K_{e3} events are 70% unique and for values of $\cos\theta_l^*$ between -0.5 and -1, there are few ambiguous events. The success of the ambiguity assignment depends on this fact, and since it is true for all regions of the K_{e3}^0 Dalitz plot, requiring isotropy in the $\cos\theta_l^*$ distribution is a powerful constraint. The falloff of the $\cos\theta_l^*$ distribution near $\cos\theta_l^* = -1$ is filled in by the correction for loss of slow leptons.

Since our experiment is done with a unique beam momentum, there is a one-to-one correspondence between the pion kinetic-energy values calculated for a $K_{\mu 3}$ or K_{e3} hypothesis, so the $K_{\mu 3}$:K_{e3} ambiguity resolution does not significantly change the pion c.m. kinetic-energy value. The spread in the beam energy introduces an uncertainty of ~5 MeV in T_π.

In order to handle the ambiguities between the charged modes, we used the constraint that there should be equal numbers of $\pi^+ l^- \nu$ and $\pi^- l^+ \nu$ events, and that they should have the same distribution on the Dalitz plot. The ratio R of the number of events in the $\pi^+ l^- \nu$ channel, $X_+(T_{\pi^+}, T_{l^-})$, to the number of events in the $\pi^- l^+ \nu$ channel, $X_-(T_{\pi^-}, T_{l^+})$, can be predicted given values for the form factors. For each event in a given bin, which is ambiguous between charge modes, we found the number of unique events in that bin, $U_+(T_{\pi^+}, T_{l^-})$, the number of ambiguous events, $A_+(T_{\pi^+}, T_{2^-})$, and the corresponding quantities $U_-(T_{\pi^-}, T_{l^+})$, $A_-(T_{\pi^-}, T_{l^+})$, and solved for the weights applied to the ambiguous events subject to the condition that

$$R = \frac{X_+(T_\pi, T_l)}{X_-(T_\pi, T_l)} = \frac{U_+(T_\pi, T_l) + w_+ A_+(T_\pi, T_l)}{U_-(T_\pi, T_l) + (1 - w_+) A_-(T_\pi, T_l)} .$$

As stated above, R depends weakly on the values of the form factors. Therefore, these weights were calculated in an iterative manner. Again, this constraint is applied bin by bin over the Dalitz plot and because of the reciprocity between the $\pi^+ e^- \nu$ and $\pi^- e^+ \nu$ systems, the technique does not, to first order, result in a distorted event distribution on the Dalitz plots.

We have also made corrections for the few events which uniquely fit a false hypothesis. These corrections, which are less than 3%, are made by generating a Monte Carlo sample of events, processing them through the same kinematic fitting programs as the data and subtracting or adding them to the appropriate data sample.

Radiative corrections were applied using the formulation of Ginsberg.[8] For photons with energies less than 1 MeV, Ginsberg gives explicit correction factors. For photon energies greater than 1 MeV, we generated Monte Carlo events of the type $K_L^0 \to \pi l \nu \gamma$, passed them through the analysis chain, and repopulated the Dalitz plots accordingly.

V. RESULTS

The weighting procedure outlined above leaves a total of 13 748 ± 186 $\pi\mu\nu$ events and 19 201 ± 227 $\pi e \nu$ events, corresponding to a branching ratio of 0.716 ± 0.008. However, since we have cut the K_{e3}^0 Dalitz plot at $T_e^* < 40$ MeV, a correction is needed. The correction factor is weakly dependent on the value of λ_+ and for a λ_+ value of 0.028, the correction factor is 0.980. This gives a final branching-ratio result $\Gamma(K_{\mu 3}^0)/\Gamma(K_{e3}^0)$ of 0.702 ± 0.008 in agreement with the world average of 0.695 ± 0.011.[3]

In order to determine the form factors λ_+ and λ_0, the data were fit in four ways and the results are summarized in Table IV. The values of uncertainties in parentheses are the statistical errors, i.e., the changes needed in the parameters to lower the logarithm of the likelihood function by 0.5 units. The second errors, as shown in Table IV, include, in addition to the statistical error, the estimated systematic effects. These systematic errors were estimated by observing how much each of the following changed the fitted parameters: (1) changing the scan efficiency numbers in Table II by one standard deviation, (2) allowing the number of events in each bin of $\cos\theta_{\text{lepton}}^*$ to vary by one standard deviation, and (3) removing the correction for events which uniquely fit a false hypothesis. The total errors were calculated by adding the systematic plus statistical uncertainties in quadrature.

The first fit in Table IV uses only the branching-ratio measurement. This is insensitive to λ_+, and we fitted only for λ_0, repeating the fit for three values of λ_+. With a value of $\lambda_+ = 0.028$, which is close to the world average, we obtained $\lambda_0 = 0.041 \pm 0.008$. Next, we fitted the $K_{\mu 3}$ Dalitz-plot density allowing both λ_+ and λ_0 to vary. This fit gave $\lambda_0 = 0.050 \pm 0.008$, which is in agreement with the branching-ratio value. We have also fitted the K_{e3}^0 Dalitz plot for λ_+ and the result, $\lambda_+ = 0.029 \pm 0.005$, agrees with our previous measurement of $\lambda_+ = 0.025 \pm 0.005$ using the unique K_{e3}^0 events only.[1] Finally, we made a simultaneous fit to both the $K_{\mu 3}$ and K_{e3} Dalitz-plot densities and the branching ratio and obtained our final values of $\lambda_+ = 0.028 \pm 0.007$ and $\lambda_0 = 0.046 \pm 0.006$. The larger error on λ_+, given by this fit over the K_{e3}^0 analyses, represents the small systematic inconsist-

TABLE IV. Results of fits to λ_+ and λ_0. The error values in parentheses are the statistical errors. The second error number includes the estimated systematic effect added in quadrature to the statistical error.

Fit		λ_+	λ_0
1	$\Gamma(K_{\mu3}/K_{e3})$	0.018 Input	0.038 ± (0.005)0.008
		0.028 Input	0.041 ± (0.005)0.008
		0.038 Input	0.043 ± (0.005)0.008
2	$K_{\mu3}$ Dalitz plot	0.028 ± (0.008)0.010	0.050 ± (0.005)0.008
3	K_{e3} Dalitz plot	0.029 ± (0.003)0.005	
4	$\Gamma(K_{\mu3}/K_{e3})$ and Dalitz plots combined	0.028 ± (0.003)0.007	0.046 ± (0.004)0.006

encies between the different techniques for measuring this parameter. Figure 4 shows the weighted T_π and T_{lepton} distributions with the curve representing the results of the final fit. The fits give $\chi^2/\text{DF} = 1.1$ for T_π from $K_{\mu3}$, 2.2 for T_μ, 2.0 for T_π from K_{e3}, and 1.8 for T_e. The magnitude of these χ^2/DOF reflect the fact that only statistical uncertainties are included in the T_π and T_{lepton} distribution.

VI. DISCUSSION

The results of these fits are compared in Fig. 5 with the world-average values of λ_+ and λ_0 determined by $K_{\mu3}^0$ Dalitz-plot analyses and the $K_{\mu3}^0/K_{e3}^0$ branching-ratio measurements.[3] The values we obtain for λ_+ and λ_0 are in excellent agreement with other measurements based on the $K_{\mu3}^0/K_{e3}^0$ branching ratio and the K_{e3}^0 Dalitz plot.[3] Our value of λ_0

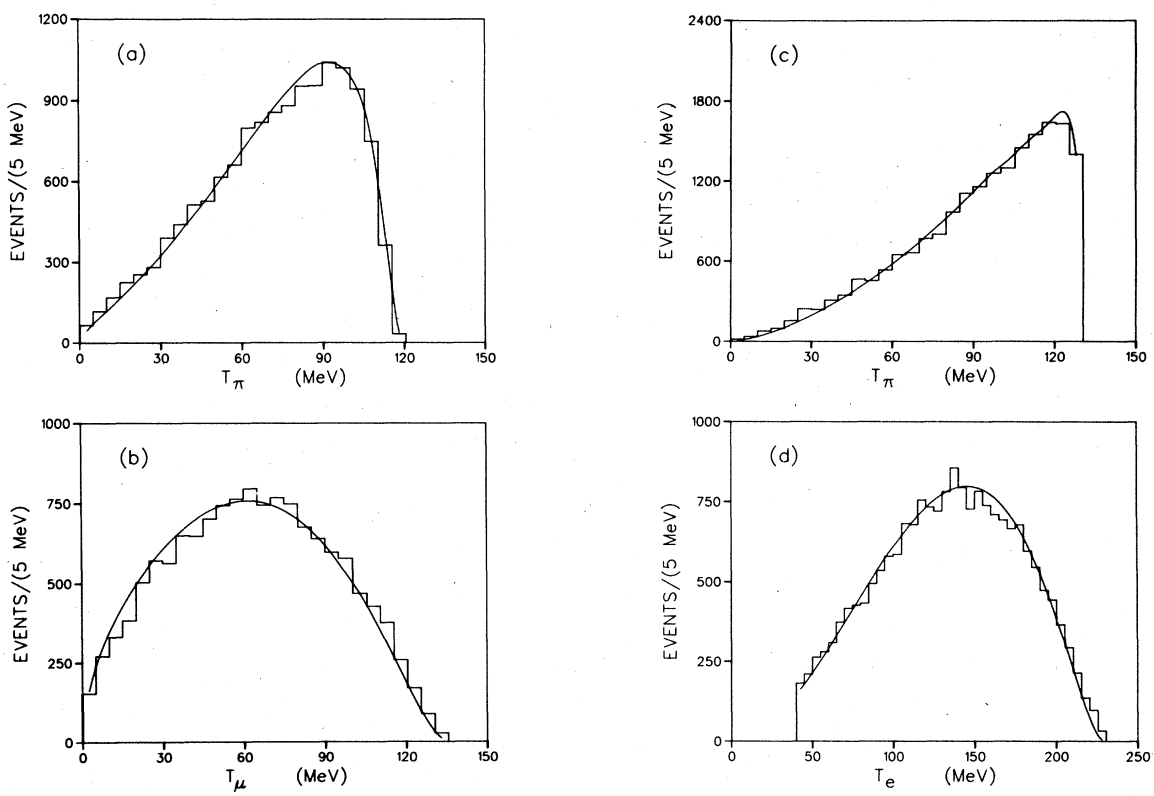

FIG. 4. (a) The distribution of weighted events in the $K_{\mu3}^0$ decay mode in T_π. The curve shows the predictions of fit 4 from Table IV. (b) Same as (a) but for T_μ. (c) The distribution of weighted events in the K_{e3} decay mode in T_π and (d) the distribution in T_e. The curves are also from fit 4.

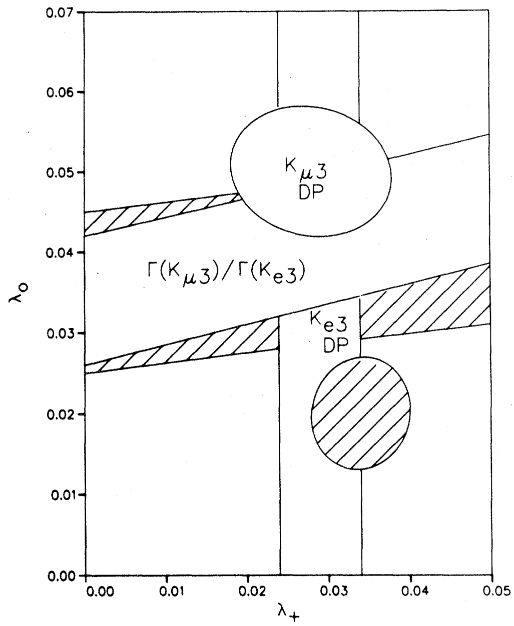

FIG. 5. The results of fits 1–3 in Table IV for λ_+ and λ_0. Also shown as shaded areas are the world-average values of previous experiments. The band represents the branching-ratio results and the ellipse the values measured from $K^0_{\mu3}$ Dalitz plot.

$= 0.050 \pm 0.008$, obtained from the $K^0_{\mu3}$ Dalotz-plot analysis, is somewhat larger than the result given by previous $K^0_{\mu3}$ Dalitz-plot experiments.

The world-average measurement for λ_+ and λ_0 from the $K^0_{\mu3}$ Dalitz plot, shown by the hatched ellipse in Fig. 5, is dominated by three high-statistics experiments.[9] The internal consistency of these experiments is satisfactory for λ_+ but not for λ_0.[2] The parameter λ_0 can also be measured from an analysis of the muon polarization and we note that the most recent experiment[10] gives a value of $\lambda_0 = 0.044 \pm 0.008$ in good agreement with our result.

In summary, our measurement of the decay parameters λ_+ and λ_0 give a consistent picture, but since we find $\lambda_0 > \lambda_+$, our results are not in agreement with the simple pole model.

ACKNOWLEDGMENTS

We would like to thank the crew of the 12-foot chamber at Argonne as well as the staff of the ZGS. We also appreciate the efforts of the personnel at both institutions. This work was supported by the U. S. Department of Energy.

---

*Present address: Michigan State University, East Lansing, Michigan 48823.
†Present address: General Electric, Medical Systems Division, Milwaukee, Wisconsin 53201.
‡Present address: Brookhaven National Laboratory, Upton, New York 11973.

[1]A. Engler *et al.*, Phys. Rev. D 18, 623 (1978).
[2]See, for example, the review by L. Pondrom, in *Particles and Fields* '76, proceedings of the Annual Meeting of the Division of Particles and Fields of the APS, edited by H. Gordon and R. F. Peierls (BNL, Upton, New York, 1977).
[3]Particle Data Group, Phys. Lett. 75B, 1 (1978).
[4]C. G. Callan and S. B. Treiman, Phys. Rev. Lett. 16, 153 (1966).
[5]L.-M. Chounet, J. M. Gaillard, and M. K. Gaillard, Phys. Rep. 4C, 199 (1972).
[6]Y. Cho *et al.*, Phys. Rev. D 15, 587 (1976).
[7]A. Engler *et al.*, Phys. Rev. D 18, 3061 (1978).
[8]E. Ginsberg, Phys. Rev. D 1, 229 (1970).
[9]K.-F. Albrecht, Phys. Lett. 48B, 393 (1974); C. D. Buchanan *et al.*, Phys. Rev. D 11, 457 (1975); G. Donaldson *et al.*, *ibid.* 9, 2960 (1974).
[10]A. R. Clark *et al.*, Phys. Rev. D 15, 553 (1977).